Singlet−Singlet and Triplet−Triplet Energy Transfer in Bichromophoric Peptides

W. G. McGimpsey,*,† L. Chen,† R. Carraway,‡ and W. N. Samaniego†

Department of Chemistry and Biochemistry, Worcester Polytechnic Institute, and University of Massachusetts Medical Center, Worcester, Massachusetts 01609

Received: January 12, 1999

Intramolecular singlet−singlet (SSET) and triplet−triplet (TTET) energy transfer processes were studied in solution in two bichromophoric peptides using absorption, fluorescence, phosphorescence, laser flash photolysis, and molecular modeling/dynamics. Compound **I**, a dipeptide formed by coupling 2-naphthyl-L-alanine and 4′-benzoyl-L-phenylalanine (naphthalene and benzophenone chromophores), undergoes intramolecular SSET from the naphthyl chromophore to the benzophenone chromophore as indicated by singlet lifetime measurements as well as a reduction in the intensity of the steady-state fluorescence emission relative to 2-naphthyl-L-alanine itself. Results of the lifetime experiments coupled with modeling studies suggest that SSET is consistent with a Förster mechanism, although other mechanisms cannot be ruled out. Low-temperature phosphorescence and room-temperature laser flash photolysis results indicate that intramolecular TTET from the benzophenone group to the naphthyl moiety proceeds with a rate constant, $k > 10^8$ s^{-1} (lower limit). Compound **II** consists of the same two chromophores appended to the backbone of a 14-residue peptide in which the chromophores are separated by two alanine−α-aminoisobutyric acid−alanine tripeptides and each end of the peptide is capped with an identical tripeptide. Circular dichroism measurements and molecular modeling/molecular dynamics calculations demonstrate an α-helical secondary structure for this peptide in acetonitrile solvent. Intramolecular SSET is again suggested by steady-state and lifetime measurements and, in this case, only the Förster mechanism is required to account for the observed rate. Laser flash photolysis measurements in acetonitrile and 50:50 ethanol/methanol again give evidence for rapid intramolecular TTET, with $k > 10^8$ s^{-1}. In contrast, phosphorescence spectra of **II** in methyltetrahydrofuran and 50:50 ethanol/methanol exhibit strong benzophenone emission consistent with inefficient TTET. This behavior is attributed to the ability of the low-temperature matrix to prevent the chromophores from achieving conformations conducive to good orbital overlap.

Introduction

Many reports of intramolecular charge and energy transfer in polychromophoric molecules have focused on understanding the effects of molecular conformation, interchromophore distance, and the bridging architecture on transfer rates[1] and have led to a greater understanding of the mechanisms of transfer. Intramolecular transfer in bichromophoric molecules is now understood to involve either a through-bond exchange mechanism or through-space (through solvent) mechanisms. Bichromophores possessing bridges that consist of rigid saturated hydrocarbon structures typically undergo efficient transfer via a super exchange through-bond mechanism.[1] Thus, cyclohexane, *trans*-decalin, steroidal, norbornyl, and other similar bridges all promote rapid through-bond transfer. Transfer rates can be especially high when the saturated bonds are held in an *all-trans* arrangement because this conformation facilitates efficient orbital overlap. In molecules where the chromophores are flexibly linked, transfer is generally regarded as a through-space process. In the case of energy transfer, the exchange mechanism (Dexter) dominates at small chromophore separations and a dipole-induced dipole mechanism (Förster) controls the rate at larger separations. The recognized distance dependences of Förster and Dexter mechanisms and the possibility of superexchange transfer have led to the use of transfer processes as probes of molecular structure. Thus, in peptides and proteins, fluorescence resonance energy transfer [FRET (Förster)] has been employed to probe and identify different structural domains with a view to understanding structure−function relationships.[2] (It should be noted that there are several limitations to using FRET for elucidating structure, including the difficulty of distinguishing between conformational changes in the chromophores and those of the protein itself.)

There are several recent studies of intramolecular transfer processes [charge transfer and singlet−singlet (SSET) energy transfer (FRET) in peptides].[3] For example, Fox observed intramolecular electron transfer in a peptide containing 14 residues with pyrene and *N*,*N*-dimethylaniline chromophores attached to the fourth and 11th residues in the chain.[3b,c] With this structure, in aprotic media, a helical domain is likely between the chromophores even if there is unfolding of the helix near the termini. Meyer et al. reported charge separation in spatially ordered polychromophoric helical oligopeptides made up of 13 to 27 proline residues.[3d,e] In a limited fashion, Sisido and co-workers[3f] studied the effects of chromophore position on electron transfer in bichromophoric peptides constructed with 0, 1, or 2 alanine residues separating naphthalene and *N*,*N*-dimethylaniline chromophores. They concluded that in these systems a through-space electron-transfer mechanism was operative. Also, Pispisa et al.[3g,h] have reported SSET in shorter bichromophoric peptides in which a terminal naphthyl-substituted lysine residue is separated from a protoporphyrin-

† Worcester Polytechnic Institute.
‡ University of Massachusetts Medical Center.

10.1021/jp9901592 CCC: $18.00
Published on Web 07/16/1999

substituted lysine by up to four residues. These studies included a theoretical investigation of peptide conformations that was subsequently used to conclude that SSET followed a Förster mechanism.

Each of these studies has contributed to an understanding of how intramolecular transfer processes can be used to determine peptide structure. From a different point of view, they have also demonstrated the potential utility of using the helical secondary structure of some peptides as scaffolds for the fabrication of molecular scale devices that would rely on efficient and predictable charge and energy conduction.[4]

With these previous studies and potential applications in mind and recognizing that most of the work in peptides so far has involved charge transfer and singlet energy transfer, we have undertaken a study of SSET and triplet−triplet (TTET) energy transfer in bichromophoric peptides. We report here our initial results for two peptides (**I** and **II**) that contain as chromophores, naphthalene and benzophenone. Compound **I** is the dipeptide formed by coupling 2-naphthyl-L-alanine and 4-benzoyl-L-phenylalanine, whereas II is a 14-residue helical peptide with the same backbone as that used by Fox et al.[3b,c] with the chromophores attached at the fourth and 11th residues. Literature reports document the tendency of bichromophores containing aromatic and ketone chromophores (such as benzophenone and naphthalene) to undergo a series of intramolecular photophysical steps upon excitation, starting with SSET from the aromatic group to the ketone moiety, followed by efficient ISC in the ketone, and finally TTET back to the aromatic group.[5] By using this pair of chromophores it was our intention to obtain kinetic information for both singlet and triplet transfer processes from the same peptide. Fluoresence spectral and lifetime measurements coupled with phosphorescence and laser flash photolysis results confirm the occurrence of the expected SSET and TTET behavior and yield approximate rate constants for the processes.

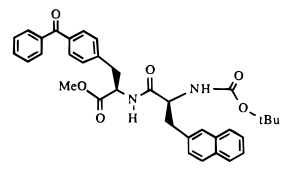

I

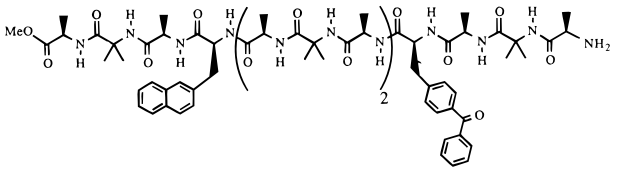

II

Experimental Section

Materials and Supplies. All solvents used in spectroscopic studies were Aldrich spectrophotometric grade and were used as received. Fmoc-3-(2-naphthyl)-L-alanine and Fmoc-(4′-benzoyl)-L-phenylalanine were used as received from Advanced ChemTech. BOC-3-(2-naphthyl)-L-alanine (SIGMA) was also used without further purification. BOC-(4′-benzoyl)-L-phenylalanine (Advanced ChemTech) was transformed to the corresponding methyl ester hydrochloride in one step.

(4′-Benzoyl)-L-phenylalanine Methyl Ester Hydrochloride. BOC-(4-benzoyl)-L-phenylalanine (0.3804 g, 1.0 mmol) was placed in a flask under nitrogen and dissolved in a mixture of 8 mL of 2,2- dimethoxypropane and 1 mL of HCl 37%.[6] The solution was stirred for 18 h, during which time it changed to a dark brown color. After that period, the solvent was eliminated, and a brownish oil was recovered. The oil was dried under vacuum for 2 h and dissolved in 5 mL methanol, and then anhydrous ethyl ether was added drop by drop, while stirring, until permanent cloudiness was evident. The mixture was allowed to stand at room temperature for a few hours, until the precipitation was complete. The solid was filtered off and dried under vacuum (0.2578 g, 0.81 mmol, 81% yield). ^{1}H NMR confirmed the complete removal of the BOC group and the formation of the methyl ester. The product was used without further purification.

Synthesis of BOC-3-(2-naphthyl)-L-alanyl-(4′-benzoyl)-L-phenylalanine Methyl Ester. (Dipeptide I). (4′-Benzoyl)-L-phenylalanine methyl ester hydrochloride (0.2200 g, 0.69 mmol) was suspended in $CHCl_3$ (4 mL) under nitrogen, cooled in an ice-water bath, and neutralized with 0.5 mL (3.6 mmol) of dry triethylamine. Then, 1-hydroxy-1*H*-benzotriazole (0.1120 g, 0.82 mmol), a solution of BOC-3-(2-naphthyl)-L-alanine (0.2190 g, 0.69 mmol) in $CHCl_3$ (8 mL), and 1-[3-(dimethylamino)propyl]-3-ethylcarbodiimide hydrochloride (EDC, 0.1580 g, 8.2 mmol) were successively added to the initial solution while maintaining the inert atmosphere. The mixture was allowed to reach room temperature and was then stirred for 18 h. After this period, the solution was diluted with $CHCl_3$ (5 mL) and washed with 1 N HCl, saturated aqueous $NaHCO_3$, and brine. The organic phase was dried over Na_2SO_4, and the solvent was evaporated with a rotary evaporator. The crude product (0.4003 g, 0.69 mmol) was dissolved in the minimum amount of methanol and slowly precipitated with water. The precipitate was filtered off, washed with a 1:1 methanol/water solution, and dried under vacuum (0.2641 g, 0.46 mmol). Final purification was performed by flash chromatography with silica flash, using dichloromethane/hexane as solvent. mp 152−154 °C; ^{1}H NMR ($CDCl_3$): 1.38 (s, 9H, *t*-Bu), 3.06−3.24 (m, 4H, 2 CH_2), 3.54 (s, 3H, $-OCH_3$), 4.43 (wd, 1H, CH, $J = 4$ Hz), 4.80 (m, 1H, CH), 5.03 (m, 1H, NH), 6.34 (d, 1H, NH, $J = 4$ Hz), 7.01 (d, 2H, Ar), 7.34−7.79 (m, 14H, Ar). ^{13}C NMR ($CDCl_3$): 28.22 (*t*-Bu), 37.88 (CH_2), 38.39 (CH_2), 52.36 (2 CH_2), 53.12 (OCH_3), 125.83, 126.27, 127.54, 124.64, 128.07, 128.29, 128.53, 129.18, 129.97, 130.31, 132.39, 167.61 (CO), 168.9 (CO), 175.9 (t-Bu*C*O), 195.93 (Ph-*C*O−Ph).

*Synthesis of MeO−Ala-Aibn-Ala-naphthylAla-(Ala-Aibn-Ala)$_2$-benzophenonylAla-Ala-Aibn-Ala (Peptide **II**).* Fmoc-3-(2-naphthyl)-L-alanine and Fmoc-(4′-benzoyl)-L-phenylalanine were obtained from Advanced ChemTech and were used without further purification. The peptide was synthesized on a 50 μmol scale using an automated Rainin Symphony synthesizer with NMBA resin, Fmoc amino acids, and HBTU-activation in the presence of 4-methyl-morpholine. Double couplings were perfomed in dimethylformamide using a 5-fold excess of reagent and a reaction time of 20 min. Deprotection was achieved using 20% piperidine for 9 min. Cleavage of the assembled peptides from the resin was performed with 86% trifluoroacetic acid, 5% H_2O, 5% anisole, 2% triisopropylsilane, 1% thiophenol, and 1% ethanedithiol. Peptides were precipitated and washed using 0 °C diethyl ether, dissolved in water, and lyophilized. The resulting powders were dissolved in ∼10 mL of acetonitrile, and water was added to maintain the solution. Chromatography was performed on a 10 × 25 cm column of μ-Bondapak C18 (Waters) using a linear gradient to 75% acetonitrile and a flow rate of 6 mL/min. Eluted peptides were identified by their absorbance at 300 nm, and their constituent amino acids were determined after hydrolysis in 6 N HCl at 150 °C for 1.5 h. Amino acid analysis was performed with the Accutag system

using Millenium software for quantitation of HPLC-identified peaks (Waters). The peptide gave integral molar ratios of the appropriate constituent amino acids.

Spectroscopic Methods. *Absorption and Fluorescence Emission Spectroscopy.* Ground-state absorption spectra and extinction coefficients were obtained with a Shimadzu 2100U absorption spectrometer. Fluorescence emission spectra were measured in nitrogen- and air-saturated acetonitrile and were found to be independent of saturating gas. Spectra were recorded with a Perkin-Elmer LS-50 spectrofluorimeter. Phosphorescence spectra were recorded with the same instrument using nitrogen-saturated methyltetrahydrofuran (MTHF) and 1:1 ethanol/methanol glasses samples were studied at 77 K. Fluorescence lifetimes were measured using a PTI single photon counting apparatus employing a H_2 lamp. All samples were nitrogen-saturated. Emission wavelengths varied according to the sample. A minimum of 10,000 counts was obtained for each sample.

Laser Flash Photolysis. The laser flash photolysis system has been described in detail elsewhere.[7] Briefly, for kinetic studies and transient absorption spectra, solutions were prepared at concentrations sufficiently large to give absorbances in the range 0.1−0.5 at the excitation wavelength. Both flowing and static samples were used. Static samples were outgassed with nitrogen in 1 cm path length quartz cuvettes and sealed prior to irradiation. Flow samples, contained in a reservoir, were continuously purged with a stream of nitrogen and were caused to flow through a specially constructed quartz cell (1 × 1 cm) with a peristaltic pump. This procedure ensured that a fresh volume of solution was exposed to each laser pulse, thereby avoiding accumulation of any photoproducts. Samples were irradiated with the pulses of a Lumonics EX 510 excimer laser (308 nm; ∼ 20 mJ/pulse; 8 ns pulse duration) or the frequency-tripled output of a Continuum Nd:YAG laser (355 nm, ∼30 mJ/pulse, 5 ns).

Circular Dichroism. Circular dichroism (CD) spectra were recorded with a AVIV Model 62DS Circular Dichroism Spectrometer. Spectra were recorded at 15 and 25 °C in acetonitrile, 85:15 acetonitrile/water, and 50:50 ethanol/methanol solvents.

Calculations. To obtain minimum energy conformations of the peptides, conformational space was explored using ChemPlus 1.5 and the MM+ force field. The lowest energy conformations were further minimized using AM1 and PM3 parameters in the Hyperchem semiempirical option. These minimized conformations were then used to obtain the spectroscopic energies with ZINDO/S parameters.

Results and Discussion

Spectroscopy of Compound I. *Bichromophoric Dipeptide. Absorption Spectra.* Figure 1 shows the molar absorption spectrum (extinction coefficients) determined for **I** as well as the composite spectrum obtained by adding the spectra of the two model compounds, 2-naphthyl-L-alanine (**III**) and 4-benzoyl-L-phenylalanine (**IV**); that is, the individual chromophores in **I**. The composite spectrum almost exactly matches the spectrum obtained for **I**, indicating little if any electronic interaction between the chromophores in the ground state. ZINDO/S calculations confirm that (i) the highest three occupied molecular orbitals and the lowest three unoccupied molecular orbitals are localized on the individual chromophores and (ii) the *relative* energies for the HOMO−LUMO transitions in the bichromophore are consistent with experimental absorption spectra of the models. Therefore, it is likely that excitation of the localized ground state of one of the chromophores initially

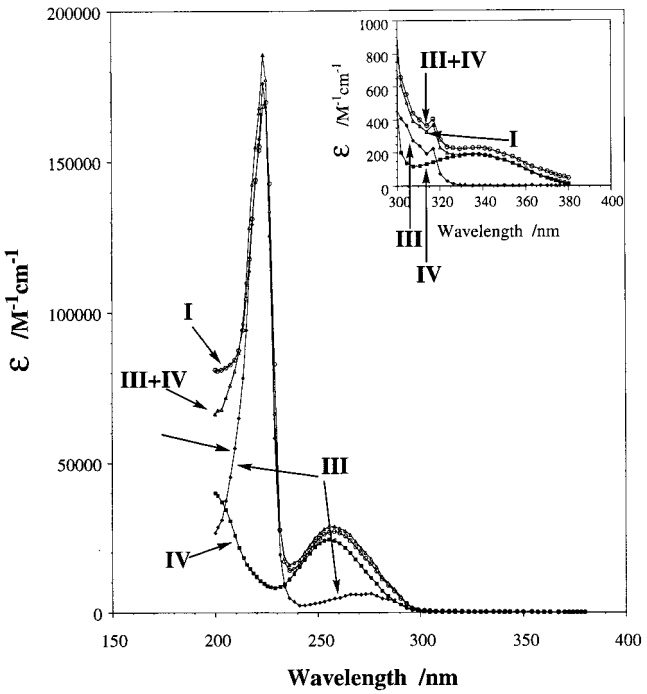

Figure 1. Molar absorption spectra of **I**, **III**, and **IV** in acetonitrile and comparison of **I** with the sum of its constituent chromophores − **III** + **IV**. Inset: Spectra above 300 nm.

will result in the production of an excited state that is localized on the same chromophore. As a result, the ratio of extinction coefficients of **III** and **IV** at any given excitation wavelength can be taken as an accurate representation of the ratio of excited states for each chromophore *initially* formed upon excitation.

Fluorescence Spectra and Lifetimes. Table 1 gives the fluorescence integrated intensities and lifetimes measured for **I** and **III** in nitrogen-saturated acetonitrile, and Figure 2 shows the emission spectra for **I** and **III** obtained at λ_{ex} 308 nm. At all excitation wavelengths, the emission spectra of **I** were identical in band shape to the spectrum of **III** and were quite similar to the spectrum of naphthalene. This result in itself is not surprising given the nonemissive nature of the benzophenone singlet state. However, the intensity of the emission was substantially smaller for **I** than for **III**, even when the absorption of **III** at the excitation wavelength was adjusted to match the absorption for the naphthyl chromophore in **I** at that wavelength (as predicted from the extinction coefficient data). The degree to which the emission intensity was attenuated in **I** relative to **III** expressed as a ratio of intensities, I_{III}/I_I, is given in Table 1 for three excitation wavelengths. These wavelengths were chosen because they provide three distinctly different excitation conditions. Thus, at 308 nm, roughly 70% of the exciting light is absorbed by the naphthalene chromophore, whereas at 226 and 260 nm, this percentage is 94 and 17, respectively. Results for each wavelength are quite similar and indicate that the emission of the naphthalene chromophore undergoes an attenuation of roughly a factor of 7 when incorporated into the dipeptide. This observation gives weight to the suggestion that the naphthyl singlet state in **I** is quenched by the benzophenone group. The nature of the quenching process could not be confirmed directly from these fluorescence studies; however, we assign it to SSET based on the thermodynamic feasibility of the process, on subsequent results from phosphorescence and laser studies (vide infra), and on literature precedent.[1(h,i,u),5] We conclude that this SSET quenching is intramolecular in nature because the concentration of **I** used in the fluorescence experi-

TABLE 1: Extinction Coefficients, Fluorescence Emission Intensities and Lifetime Data for I−IV

λ	variable	I	II	III	IV
226 nm	ϵ (M^{-1} cm^{-1})			150 030	8 630
	$I^{a,b}$	915	2250	6 500	
	$I_{III/II}$	7.1			
	$I_{III/III}$		2.8		
260 nm	ϵ (M^{-1} cm^{-1})			4 850	23 300
	$I^{a,b}$	910	2470	6 205	
	$I_{III/II}$	6.8			
	$I_{III/III}$		2.5		
308 nm	ϵ (M^{-1} cm^{-1})			270	120
	$I^{a,b}$	890		6 450	
	$I_{III/II}$	7.2			
290 nm	τ (ns); A[c]; (χ^2)	$\tau_1 = 33.27 \pm 0.08$ $A_1 = 0.658 \pm 0.003$ $\tau_2 = 2.62 \pm 0.07$ $A_2 = 0.342 \pm 0.023$ (1.9)	$\tau_1 = 40.97 \pm 0.06$ $A_1 = 0.075 \pm 0.015$ $\tau_2 = 14.22 \pm 0.06$ $A_2 = 0.253 \pm 0.011$ $\tau_3 = 2.41 \pm 0.07$ $A_3 = 0.672 \pm 0.016$ (1.5)	$\tau_1 = 70.05 \pm 0.12$ $A_1 = 1.000 \pm 0.014$ (2.1)	

[a] Relative intensities. [b] Integrated intensity, **I**, was corrected by accounting for the difference in naphthyl absorbance in **I** or **II** versus **III**, as expected from the extinction coefficients of **III** and **IV**; e.g., $I_I(\lambda)$ (corrected) = $I_I(\lambda)$ (measured) x $(I_{III} + I_{IV})/I_{III}$. [c] Preexponential factor.

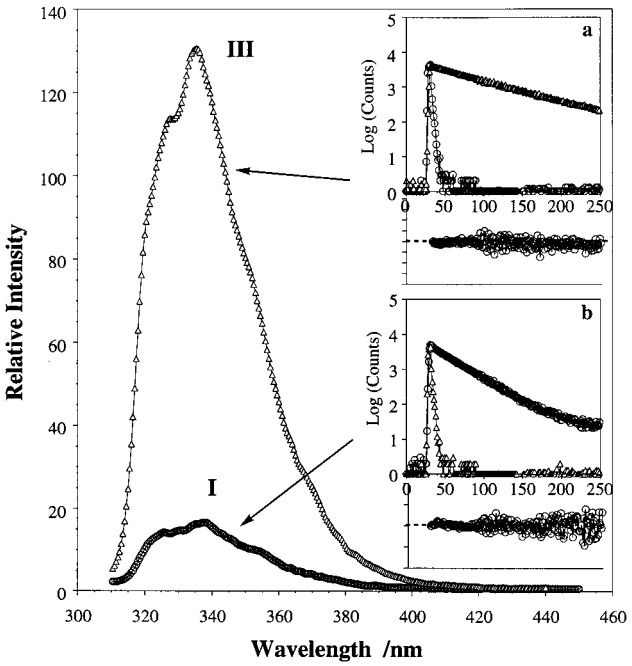

Figure 2. Fluorescence emission spectra of **I** and **III** in nitrogen-saturated acetonitrile at λ_{ex} 226 nm. Insets: Single photon counting decay profile obtained in nitrogen-saturated acetonitrile at λ_{ex} 290 nm for (a) **III** and (b) **I**. Time scale for insets is ns. Residuals are shown for both insets. Range of residuals scales are −0.2−0.2 in both cases.

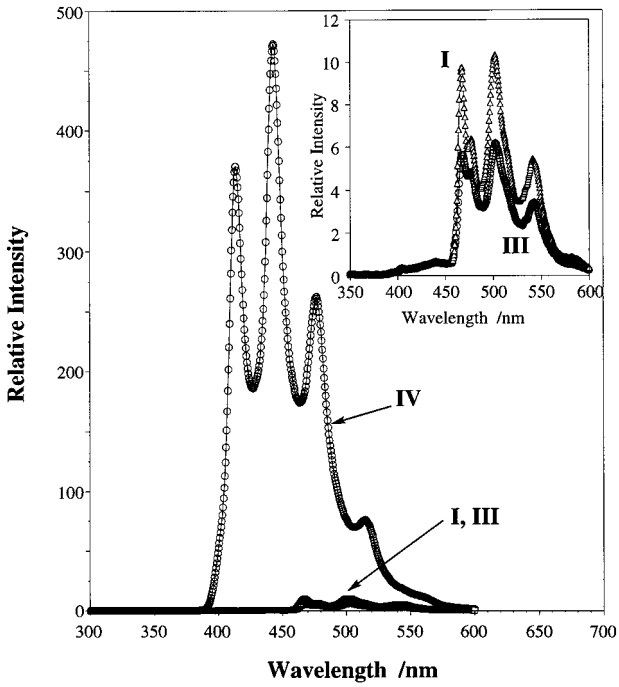

Figure 3. Phosphorescence emission spectra for **I**, **III**, and **IV** obtained in nitrogen-saturated 50:50 ethanol/methanol 77 K glass with λ_{ex} 290 nm. Inset: Spectra of **I** and **III**.

ments is too low ($<10^{-4}$ M) and the lifetime of the naphthyl singlet state as determined for **III** (∼70 ns, vide infra) is too short to allow efficient intermolecular quenching. To confirm this, the emission spectrum was obtained for an equimolar mixture of models **III** and **IV** at concentrations similar to that used for **I**. Little effect was observed on the intensity of emission.

Singlet lifetime measurements also provide evidence for intramolecular quenching. The decay of the fluorescent state of **I** can be represented by two exponentials, whereas the decay of **III** follows a single exponential [lifetimes (τ), preexponential factors (A), and χ^2 values are given in Table 1]. The insets in Figure 2 show the decay profiles for **I** and **III**, and the residuals are shown. The fluorescence quenching efficiency as indicated from the lifetimes is qualitatively consistent with the attenuated emission intensity observed. However, because of the multiexponential behavior of the fluorescence of **I**, in a discussion of the energy transfer mechanism, we have calculated the energy transfer efficiency from the time-resolved data and not from the steady-state results (vide infra).

Phosphorescence Spectra. Figure 3 shows the phosphorescence spectra of **I**, **III**, and **IV** obtained in nitrogen-saturated 1:1 ethanol/methanol solution at 77 K using λ_{ex} 290 nm. The inset shows the weaker **I** and **III** emission separately. At this wavelength, approximately half of the excitation light is absorbed by each chromophore. Immediately apparent from these spectra is the lack of observed benzophenone emission in **I** and the similarity of the emission of **I** to that of the naphthyl chromophore in **III**. Clearly, the benzophenone triplet state in **I** is efficiently quenched and because diffusional interaction is expected to be very inefficient in the glass, we attribute quenching to intramolecular TTET. From the lack of observed emission for the benzophenone chromophore, a lower limit for the rate constant for TTET can be assigned − $k_{TTET} > 2 \times 10^5$

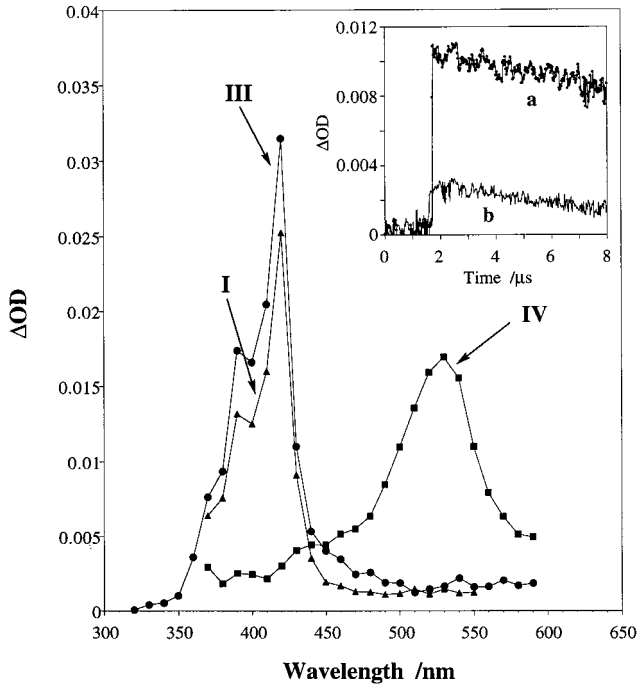

Figure 4. Transient absorption spectra of **I** and **IV** in nitrogen-saturated acetonitrile obtained 0.5 μs after 355 nm laser photolysis and for **III** under similar conditions after 308 nm laser photolysis. Inset: Growth and decay of transient absorption of **I** at 425 nm following 355 nm laser photolysis. Decay a: $[\mathbf{I}] = 6 \times 10^{-5}$ M; Decay b: $[\mathbf{I}] = 6 \times 10^{-6}$ M. The magnitude of the absorbance in decay b was multiplied by a factor of 4 to better illustrate the growth.

s^{-1}.[8] However, given the time-resolved laser results described below, it is clear that the actual rate constant is considerably larger.

Supporting the occurrence of TTET is the comparable, although somewhat higher intensity of the naphthyl phosphorescence in **I** as compared with that of **III** for samples with matching absorbance at 290 nm. In the absence of TTET, the emission intensity for **I** should be one-half that of **III** because the extinction coefficients of the naphthalene and benzophenone chromophores are roughly equal at this wavelength. The observation that the emission is comparable is consistent with efficient TTET, that is, the half of the excitation light that is absorbed by the benzophenone group is funneled back into the naphthalene triplet state. The somewhat higher intensity observed for **I** actually reflects the more efficient population of the naphthyl triplet by TTET than by ISC.

Laser Flash Photolysis. Figure 4 shows the room-temperature transient absorption spectra obtained for **I** and **IV** in nitrogen-saturated acetonitrile following 355 nm YAG laser excitation and for **III** following 308 nm excimer laser excitation. The spectrum of **I** was also obtained using 308 nm excitation and yielded similar results. From the oxygen sensitivity of the transient spectra for **III** and **IV** and their similarity to those reported in the literature,[9] they are assigned to the naphthyl and benzophenone triplet states, respectively.

Clearly, the spectrum of **I** is identical in band shape to that of **III** and for this reason is assigned as the triplet state of the naphthyl chromophore. (The difference in the actual triplet absorbances in this figure is attributed to the different excitation wavelengths.) There is no contribution to the spectrum due to the benzophenone triplet state. At 355 nm, 99% of the excitation light is absorbed by the benzophenone group and therefore formation of the naphthyl triplet state must occur as a result of excitation of the benzophenone chromophore, ISC to the triplet state and TTET to the naphthyl chromophore. The relatively long lifetime for the benzophenone triplet in solution makes it possible that this TTET process is intermolecular rather than intramolecular, especially given the higher ground-state concentrations used in the laser measurements compared with the fluorescence experiments. However, two observations argue against intermolecular transfer. First, there was no resolvable growth of the naphthalene T−T absorption (i.e., the naphthalene triplet was generated within the duration of the laser pulse). At the concentrations of **I** normally used for the 355 nm experiments (0.5−1.0 mM), intermolecular TTET should result in a growth lifetime that is well within the time resolution of our instrumentation. Second, when the concentration of I was varied from 6×10^{-4} to 6×10^{-6} M, the growth of the naphthyl triplet state was still complete within the duration of the laser pulse. We conclude from these observations as well as from the phosphorescence results that TTET from the benzophenone group to the naphthyl group is intramolecular. Figure 4 (inset) shows the decay kinetics obtained at 425 nm (the naphthyl T−T maximum) for two concentrations of **I**.

At 308 nm, roughly 30% of the exciting light is absorbed by the benzophenone moiety and 70% by the naphthyl group. Because a substantial amount of the absorption is into the benzophenone group, some naphthyl triplet formation following 308 nm excitation must occur via the same TTET process observed for 355 nm excitation. Again, if this process were intermolecular, resolvable growth kinetics would be observed. However, all of the naphthyl triplet growth is complete within the duration of the laser pulse. This behavior again strongly supports intramolecular TTET. Because a substantial amount of the excitation light is absorbed by the naphthyl group, naphthyl triplet formation must also occur by (i) excitation to the naphthyl singlet state followed by ISC to the triplet, and/or (ii) excitation to the naphthyl singlet state, intramolecular SSET to the benzophenone singlet, ISC and intramolecular TTET back to the naphthyl triplet. Because the SSET rate constant estimated from the fluorescence results is comparable to the ISC rate constant expected for the naphthyl chromophore as indicated from the literature[8] and from the fluorescence lifetime of **III**, and because emission results indicate the reasonably high efficiency of SSET, we conclude that direct excitation of the naphthyl singlet state will result in formation of the naphthyl triplet by *both* (i) and (ii). The value of the rate constants for TTET can only be assigned a lower limit from these experiments due to the time resolution of the instrumentation. Thus, we estimate $k_{TTET} > 10^8$ s^{-1}.

Spectroscopy of Compound II. *Bichromophoric Helical Peptide. Circular Dichroism.* Figure 5 shows the CD spectra of **II** in neat acetonitrile, 85:15 acetonitrile/water, and 50:50 ethanol/methanol obtained at 15 °C. The concentrations were matched for each sample. The spectrum in neat acetonitrile exhibits minima at 230 and 208 nm, features that are typically identified with a peptide possessing a right-handed helical secondary structure. The spectrum is nearly identical to those obtained by Fox and co-workers for bichromophoric peptides with backbones that are the same as those in **II**.[3b,c] As shown, addition of 15% water to the acetonitrile solution of **II** causes substantial change in the CD spectrum. From these results combined with literature precedent, we conclude that **II** possesses α-helical structure in acetonitrile but that the helix is substantially disrupted by intermolecular hydrogen bonding with water. In alcohol solvent, the spectral features associated with the helix are observed but are much less pronounced, likely indicating that the helical structure of the peptide is only partially retained.

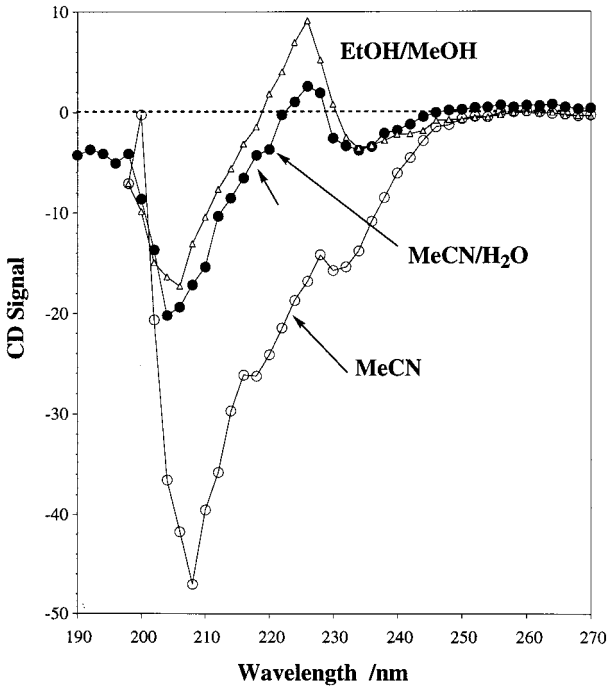

Figure 5. Circular dichroism spectra of **II** in acetonitrile, 85:15 acetonitrile/water, and 50:50 ethanol/methanol obtained at 15 °C.

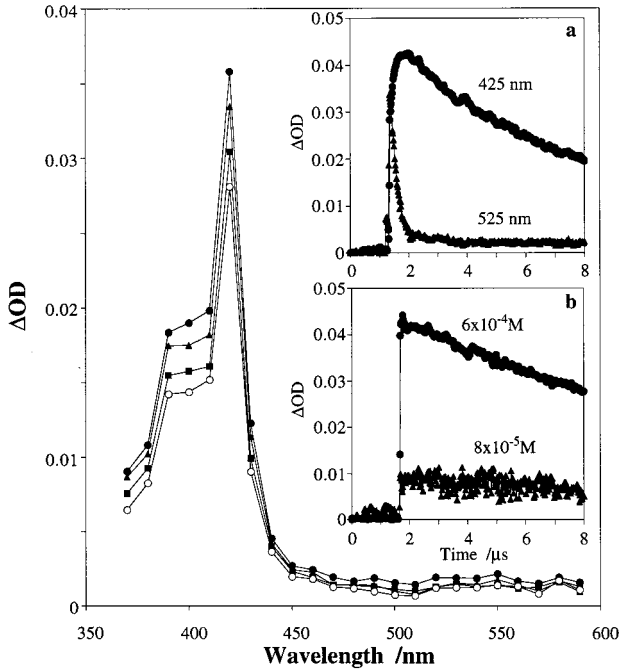

Figure 6. Transient absorption spectra of **II** in nitrogen-saturated acetonitrile obtained 0.5, 1, 2, and 4 μs after 355 nm laser photolysis. Inset a: Transient decay profiles obtained at 425 and 525 nm following 355 nm laser excitation of an equimolar mixture of **III** and **IV** (6×10^{-4} M). Inset b: Growth and decay of transient absorption of **II** at 425 nm following 355 nm laser photolysis.

Absorption Spectra. As with **I**, the absorption spectrum of **II** is similar to the sum of the spectra of **III** and **IV**. There are minor differences in the extinction coefficients but the overall band shapes are quite similar. Distinct features in the spectrum of **II** indicate the presence of both chromophores as well as the lack of interaction between the chromophores in the ground state. These features include the naphthyl peak at 226 nm and the benzophenone peak at 260 nm as well as benzophenone absorption above 300 nm. Absorption spectra of the unsubstituted amino acids (alanine and α-aminoisobutyric acid) indicated little absorption above 250 nm and only weak absorption at 226 nm, one of the wavelengths used for emission studies (vide infra). From the extinction coefficients of the amino acids at 226 nm, it is estimated that their contribution to the peptide absorption at this wavelength is <2%.

Fluorescence Spectra and Lifetimes. Excitation of nitrogen-saturated solutions of **II** at 226 nm, where the naphthalene chromophore absorbs strongly, yielded results that were qualitatively similar to those obtained for **I**; that is, the emission band shape was nearly identical to that of the naphthyl model compound **III**. As with **I**, the emission intensity of **II** was less than that of **III**, although the reduction in intensity was less pronounced for **II** than for **I** (reduction by a factor of ∼2.5 compared with a factor of 7 decrease for **I**). Identical behavior was observed at other excitation wavelengths (e.g., at 260 nm where the majority of the absorption is due to the benzophenone chromophore). Again, the reduction in fluorescence intensity is attributed to SSET from the naphthyl chromophore to the benzophenone moiety. Furthermore, the low concentration of **II** in these experiments ($<10^{-5}$ M), rules out the possibility of intermolecular interaction and therefore SSET must be intramolecular. The occurrence of SSET is also supported by fluorescence lifetime measurements. As with I, the fluorescence decay in **II** was more rapid than the decay for **III** and again, multiple exponentials were required to fit the data.

Laser Flash Photolysis and Phosphorescence. To correlate the secondary structure of the peptide with its triplet state behavior, CD, room-temperature laser flash photolysis, and low-temperature phosphorescence spectra ideally should be obtained in two solvent systems, one that is known to stabilize helical structure and one that does not. Ethanol/methanol provided adequate solubility of **II** and a good 77 K glass for phosphorescence measurements. CD measurements indicated substantial disruption of the helix in this solvent system. Acetonitrile is aprotic and does not disrupt the helix, it is optically transparent at low wavelengths, and sufficiently polar to provide good solubility for **II**. However, it does not form a suitable glass at 77 K. For this reason, ethanol/methanol and acetonitrile were used in the laser flash photolysis experiments, but acetonitrile could not be used in the phosphorescence experiments. Several other solvent systems were tested but it was not possible to identify an aprotic solvent with adequate transparency in the important 200−220 nm region of the spectrum (necessary for the CD measurements) that was also suitable for low-temperature work. Therefore, phosphorescence spectra of **II** were obtained in nitrogen-saturated methyltetrahydrofuran (MTHF) and 50:50 ethanol/methanol at 77 K with λ_{ex} 290 nm. MTHF was chosen because it forms a glass at low temperature with only minor cracking and, although its poor transparency at 220 nm prevents CD experiments, its inability to form hydrogen bonds makes it a good candidate not to disrupt helical structure.

Transient absorption spectra were obtained for **II** in nitrogen-saturated acetonitrile using both 355 nm Nd:YAG and 308 nm excimer laser excitation (Figure 6). The main feature in the transient spectrum, an intense absorption band at 425 nm that is quenched by air, strongly resembles the T−T absorption of the naphthyl chromophores in **I** and **III** and is identified as such. At 355 nm, >99% of the absorption takes place into the benzophenone group. Thus, the lack of observed benzophenone T−T absorption and the observation of naphthyl triplet absorption is strong evidence for TTET. The production of the naphthyl T−T absorption was instantaneous (i.e., within the duration of the laser pulse), indicating very rapid transfer and suggesting

an intramolecular process. However, as in the case of **I**, the ground state concentrations used were sufficiently large to make intermolecular transfer a possibility. For this reason, a concentration dependence study was conducted to determine the effect of peptide concentration on the growth of the naphthyl triplet. No concentration dependence was observed over the range [**II**] $= 6 \times 10^{-4}-8 \times 10^{-5}$ M (i.e., the growth kinetics at 425 nm were still shorter than the laser pulse duration). Because intermolecular quenching at 6×10^{-4} and 8×10^{-5} M would be expected to result in minimum growth lifetimes of ~200 ns and ~1.2 μs, respectively (given a diffusion-limited quenching rate), it is highly probable that the TTET process is intramolecular. As a further check, an equimolar solution containing 6×10^{-4} M **III** and **IV** was subjected to 355 nm laser photolysis. The growth kinetics of the naphthyl triplet and the decay kinetics of the benzophenone triplet were easily resolved under these intermolecular TTET conditions. Figure 6 insets a and b show kinetic behavior for the intermolecular control experiment involving **III** and **IV**, and the behavior at 425 nm for **II** at two concentrations, respectively. These results indicate that as in the case of **I**, intramolecular TTET in **II** is quite rapid, occurring with a minumum rate constant of 1×10^8 s^{-1}. (This represents the time resolution of the instrumentation.)

Transient spectra and kinetics were similar in ethanol/methanol. Thus, only the naphthyl triplet state was observed and its formation took place rapidly within the duration of the laser pulse. Again, there was no dependence of the growth on concentration even at concentrations expected to produce resolvable growth kinetics assuming an intermolecular TTET process. Therefore, as in acetonitrile, TTET is likely an intramolecular event. The fact that TTET is still quite rapid in this solvent system is not entirely consistent with the loss of helicity of the peptide as indicated by the CD. With such a loss of secondary structure, a slower rate could potentially be expected. However, given the very rapid rate of intramolecular TTET in other molecules containing the same two chromophores,[10] even a significantly decreased rate in ethanol/methanol that might be expected as a result of the loss of helicity and an accompanying increase in average interchromophore separation could be masked by the time resolution of the laser system.

The phosphorescence spectra of **II** in ethanol/methanol and MTHF were significantly different from the spectrum of **I** shown in Figure 3. Unlike the spectrum for **I**, the major feature in these spectra is strong benzophenone phosphorescence emission. The immediate conclusion that can be drawn from this observation, that TTET is inefficient, is inconsistent with the room-temperature time-resolved evidence that indicates intramolecular TTET is rapid. We suggest that the origin of this difference lies in the greater rotational mobility allowed in room-temperature liquid solutions compared with low-temperature glasses. The low-temperature matrices may freeze out or restrict motion of the chromophores and thereby prevent them from achieving conformations that provide the orbital overlap required for efficient exchange energy transfer. The effect of relative chromophore conformation on transfer efficiency has been reported in the past.[11] Good orbital overlap may be furnished by small interchromophore distances as well as conformations that involve stacking of the aromatic π-systems of the chromophores. However, such conformations may not be those with the lowest energies and therefore may not be achieved at low temperature. In room temperature liquid solution, relatively unhindered rotational motion will allow the chromophores to sample a wide variety of conformations possessing both good and poor overlap. As long as the rate of interconversion between the conformers is competitive with the TTET rate, more rapid transfer can be expected at room temperature. Such an explanation has been invoked to explain the dependence of SSET rates on conformation in bichromophoric peptides containing protoporphyrin and naphthalene chromophores.[3h]

SSET and TTET Mechanisms. Correlation With Molecular Structure. SSET is normally discussed in terms of Förster (dipole-induced dipole or radiative) and/or Dexter (electron exchange) mechanisms.[12] When the energy transfer process is intramolecular, a super-exchange process involving through-bond transfer may also be operative. This latter process is usually most effective when the molecular structure linking the chromophores is rigid and the bonds in the linker are *all-trans*, although through-bond electron transfer has been observed in bichromophoric molecules employing other linkers, including amides and peptides.[13,14]

The most straightforward intramolecular mechanism to evaluate is the Förster mechanism. In general, the efficiency of Förster energy transfer is given by eq 1 where R_0 is the critical Förster separation, the donor/acceptor distance at which the rates of energy transfer and the intrinsic deactivation of the donor excited state in the absence of the acceptor are the same (i.e., 50% transfer efficiency, calculated according to eq 2), and R is the actual interchromophore separation assuming that Förster transfer is the dominant transfer mechanism.[12]

$$E = \frac{1}{1 + \dfrac{R^6}{{R_0}^6}} \tag{1}$$

$$R_0 = \frac{9000 \ln(10) \kappa^2 \Phi_D}{128 n^4 \pi^5 N_A} \int_0^\infty f_D(\bar{\nu})\, \epsilon_A(\bar{\nu})\, \bar{\nu}^{-4}\, d\bar{\nu} \tag{2}$$

In eq 2, Φ_D is the fluorescence quantum yield of the donor in the absence of acceptor, n is the refractive index of the solvent, N_A is Avogadro's number, κ^2 is a term that describes the relative orientation of the transition dipoles for the donor and acceptror groups and in the case of freely rotating chromophores is usually assigned a value of 2/3, and the spectral overlap integral is calculated from $f_D(\nu)$, the emission spectrum (the integral is normalized to one), and ϵ_A, the molar absorption spectrum.

Evaluation of the Förster transfer mechanism in **I** and **II** involves determination of the transfer efficiency from fluorescence measurements, calculation of the critical Förster distance from spectroscopic data, and the use of eq 1 to obtain a value for R. Comparison of this interchromophore separation with that obtained by molecular modeling gives a qualitative evaluation of the importance of Förster transfer. The transfer efficiency can be obtained from eq 3, where k_0 is the rate constant for the observed fluorescence decay of the donor in the absence of acceptor as obtained from time-resolved measurements (**III**: $\tau = 70$ ns), and k is the decay rate constant in the presence of acceptor (see Table 1). For **I** and **II**, each of which exhibited multiexponential fluorescence decays, k was calculated from the individual lifetimes weighted according to the amplitudes of each. (In eq 4, A is the amplitude and τ is the lifetime for each of i components in the multiexponential decay.) Table 2 gives the values of k, the efficiency calculated from eq 3, the critical Förster distance, R_0, and the interchromophore separa-

TABLE 2: Calculated Parameters for the Determination of Förster Energy Transfer Efficiency

chromophore	k (s^{-1})	efficiency[a] (E)	R_0[b] (Å)	R_{calc}[c] (Å)	R_{model}[d] (Å)
I	1.51×10^7	0.91	16.1	10.9	11.7 (‘*trans*’) 4.2 (‘*cis*’)
II	3.02×10^8	0.95	16.1	9.8	10.1[e]

[a] From eq 3. [b] These values are the same because **III** and **IV** were the models for both **I** and **II**. [c] From eq 1. [d] Carbonyl-to-naphthyl (edge) separation. [e] Assuming chromophores lie perpendicular to axis of helix.

tion, R_{calc}, calculated from eq 1 for both **I** and **II**.

$$E = \frac{k - k_0}{k} \tag{3}$$

$$k = \sum_i A_i/\tau_i \tag{4}$$

That the values of R_{calc} determined for **I** and **II** by this method are substantially smaller than R_0 reflects the relatively efficient quenching of the naphthyl fluorescence in these compounds. Molecular modeling and dynamics calculations for **I** and **II** were carried out using HyperChem 5.02 (PC version, HyperCube, Inc.) to estimate the interchromophore separation for comparison with R_{calc}. (Separations calculated from these modeling studies are given as R_{model} in Table 2.) In **I**, two low-energy, rotationally differentiated structures were identified, corresponding to ‘*trans*’ and ‘*cis*’ arrangements of the two chromophores. The interchromophore distances in these structures were 13.5 Å center-to-center and 7.6 Å edge-to-edge (‘*trans*’) and 5.0 Å center-to-center and 3.9 Å edge-to-edge (‘*cis*’). Because the benzophenone singlet state acceptor is $n\pi^*$ in character and is therefore localized on the carbonyl group, perhaps a more realistic distance may be that measured from the carbonyl group to the edge of the naphthyl group (11.7 Å, ‘*trans*’; 4.2 Å, ‘*cis*’). In any event, the conformational picture that emerges from these calculations for **I** is one of a fairly broad range of possible interchromophore separations. That the R_{calc} value calculated for **I** (10.9 Å) lies within this broad range of separations gives qualitative support for the participation of the Förster mechanism in the observed SSET. However, it is not possible to rule out the participation of either through-space exchange or through-bond super-exchange mechanisms.

In modeling **II**, the peptide was constructed as an α-helix using the amino acid database supplied with the program. The naphthyl- and benzophenone-substituted alanines were originally included in the peptide as unsubstituted residues and were modified later to incorporate the chromophores. The geometries of the chromophore side chains were roughly minimized using partial molecular mechanics, charges were calculated using PM3, and finally, the complete structure was minimized using the MM+ force field. The minimized structure was subjected to a molecular dynamics study under periodic conditions for a 50 ps interval, followed by simulated annealing. Two different environments were employed − vacuum and water solvation (using the TIP3 water model). Both studies yielded similar results. The final conformations had lower energy than the starting minimized structure and the helical secondary structure was maintained. Because a general force field was employed, these results indicate a high probability that the system is a helix in solution. Of note are the relative conformations of the chromophores in the low energy structures. As expected there is a small stagger angle between the two groups (i.e., the chromophores overlap partially when the peptide is viewed along the axis of the helix). There is some indication from these calculations that the benzophenone group is bent toward the naphthyl group, which itself lies perpendicular to the helical axis. In this structure the average chromophore-to-edge distance is 9.1 Å. However, we attribute this bend to a hydrophobic response of the chromophores to the vacuum or water modeling environment. In less polar media, it is reasonable to expect a slightly larger separation consistent with both chromophores perpendicular to the helical axis (i.e., ∼10.1 Å). When compared with **I**, there is a smaller range of chromophore separations indicated by these calculations (± ∼1.5 Å from the value already given). This smaller range could have been predicted because the interchromophore distance is now controlled only by rotational motion of the chromophores themselves and the methylenic bond joining the chromophores to the peptide backbone, whereas in **I**, the entire structure has nearly barrier-free rotational motion. The separations calculated in this manner are consistent with the R_{calc} value (9.8 Å) determined assuming Förster transfer, and we conclude that for **II** there is no need to invoke another transfer mechanism.

TTET is almost exclusively regarded as an exchange process because the triplet−singlet interaction usually suffers from poor spectral overlap. Due to the requirement for good orbital overlap, exchange transfer requires close approach of donor and acceptor to have high efficiency and for interchromophore separations greater than ∼10 Å it is usually considered to be of minor importance. For **I**, the range of separations will certainly allow efficient exchange transfer and this likely accounts for the efficient TTET observed. For **II**, the range of separations is smaller and is close to 10 Å and for this reason a slower TTET could be expected. However, because the time resolution of our laser instrumentation is $\sim 10^8$ s^{-1}, it is not possible to compare the rates for the two peptides. It is also not possible to rule out the participation of a super exchange mechanism involving the intervening peptide framework that could contribute to a faster TTET than expected by through-space exchange.

Acknowledgment. The authors acknowledge the financial support of the National Science Foundation (CHE-9617830). We also thank the donors of the Petroleum Research Fund administered by the American Chemical Society for partial support of this work. We are indebted to Dr. Robert Talanian, BASF Bioresearch for use of the circular dichroism facilities and to Dr. Linda Johnston, National Research Council Canada, for use of single photon counting facilities.

References and Notes

(1) (a) Closs, G. L.; Johnson, M. D.; Miller, J. R.; Piotrowiak, P. *J. Am. Chem. Soc.* **1989**, *111*, 3751. (b) Sigman, M. E.; Closs, G. L. *J. Phys. Chem.* **1991**, *95*, 5012. (c) Closs, G. L.; Calcaterra, L. T.; Green, N. J.; Penfield, K. W.; Miller, J. R. *J. Phys. Chem.* **1986**, *90*, 3673. (d) Johnson, M. D.; Miller, J. R.; Green, N. S.; Closs, G. L. *J. Phys. Chem.* **1989**, *93*, 1173. (e) Chattoraj, M.; Bal, B.; Closs, G. L.; Levy, D. H. *J. Phys. Chem.* **1991**, *95*, 9666. (f) Morrison, H.; Pallmer, M.; Loeschen, R.; Pandey, B.; Muthuramu, K.; Maxwell, B. *J. Org. Chem.* **1986**, *51*, 4676. (g) Jiang, S. A.; Xiao, C.; Morrison, H. *J. Org. Chem.* **1996**, *61*, 7045. (h) Wu, Z.-Z.; Morrison, H. *Photochem. Photobiol.* **1989**, *50*, 525. (i) Wu, Z.-Z.; Morrison, H. *J. Am. Chem. Soc.* **1992**, *114*, 4119. (j) Wu, Z.-Z.; Nash, J.; Morrison, H. *J. Am. Chem. Soc.* **1992**, *114*, 6640. (k) Agyin, J. K.; Morrison, H.; Siemiarczuk, A. *J. Am. Chem. Soc.* **1995**, *117*, 3875. (l) Agyin, J. K.; Timberlake, L. D.; Morrison, H. *J. Am. Chem. Soc.* **1997**, *119*, 7945. (m) Oevering, H.; Paddon-Row: M. N.; Heppener, M.; Oliver, A. M.; Cotsaris, E.; Verhoeven, J. W.; Hush, N. S. *J. Am. Chem. Soc.* **1987**, *109*, 3258. (n) Oliver, A. M.; Craig, D. C.; Paddon-Row: M. N.; Kroon, J.; Verhoeven, J. W. *Chem. Phys. Lett.* **1988**, *150*, 366. (o) Clayton, A. H. A.; Ghiggino, K. P.; Wilson, G. J.; Keyte, P. J.; Paddon-Row: M. N. *Chem. Phys. Lett.* **1992**, *195*, 249. (p) Kroon, J.; Oevering, H.; Verhoeven, J. W.; Warman, J. M.; Oliver, A. M.; Paddon-Row: M. N. *J. Phys. Chem.* **1993**, *97*, 5065. (q)

Lawson, J. M.; Paddon-Row: M. N.; Schuddeboom, W.; Warman. J. M.; Clayton, A. H. A.; Ghiggino, K. P. *J. Phys. Chem.* **1993**, *97*, 13099. (r) Paddon-Row: M. N. *Acc. Chem. Res.* **1994**, *27*, 18. (s) Roest, M. R.; Lawson, J. M.; Paddon-Row: M. N.; Verhoeven, J. W. *Chem. Phys. Lett.* **1994**, *230*, 536. (t) Ghiggino, K. P.; Paddon-Row: M. N.; Craig, D. C. *J. Org. Chem.* **1997**, *62*, 3281. (u) Zimmerman, H. E.; Goldman, T. D.; Hirzel, T. K.; Schmidt, S. P.; *J. Org. Chem.* **1980**, *45*, 3933.

(2) See Weiss, S. *Science* **1999**, *283*, 1676 and references therein.

(3) (a) Batchelder, T. L.; Fox III, R. J.; Meier, M. S.; Fox, M. A. *J. Org. Chem.* **1996**, *61*, 4206. (b) Galoppini, E.; Fox, M. A. *J. Am. Chem. Soc.* **1996**, *118*, 2299. (c) Fox, M. A.; Galoppini, E. *J. Am. Chem. Soc.* **1997**, *119*, 5277. (d) Slate, S. A.; Striplin, D. R.; Moss, J. A.; Chen, P.; Erickson, B. W.; Meyer, T. J. *J. Am. Chem. Soc.* **1998**, *120*, 4885. (e) McCafferty, D. G.; Friesen, D. A.; Danielson, E.; Wall, C. G.; Saderholm, M. J.; Erickson, B. W.; Meyer, T. J. *Proc. Natl. Acad. Sci. U.S.A.* **1996**, *93*, 8200. (f) Inai, Y.; Sisido, M.; Imanishi, Y. *J. Phys. Chem.* **1991**, *95*, 3847. (g) Pispisa, B.; Venanzi, M.; Palleschi, A.; Zanotti, G. *Macromolecules* **1994**, *27*, 7800. (h) Pispisa, B.; Palleschi, A.; Venanzi, M.; Zanotti, G. *J. Phys. Chem.* **1996**, *100*, 6835.

(4) (a) Arrhenius, T. S.; Blanchard-Desce, M.; Dvolaitzky, M.; Lehn, J.-M.; Malthete, J. *Proc. Natl. Acad. Sci. U.S.A.* **1986**, *83*, 5355. (b) Kenny, P. W.; Miller, L. W. *J. Chem. Soc. Chem. Comm.* **1988**, 84. (c) Hopfield, J. J.; Onuchic, J. N.; Beraten, D. N. *Science* **1988**, *241*, 817. (d) Lehn, J.-M. *Angew. Chem., Int. Ed. Engl.* **1988**, *27*, 89. (e) Aviram, A. *J. Am. Chem. Soc.* **1988**, *110*, 5687. (f) Donovan, K. J.; Wilson, E. G. *Synthetic Metals* **1989**, *28*, D569. (g) Hush, N. S.; Wong, A. T.; Backsay, G. B.; Reimers, J. R. *J. Am. Chem. Soc.* **1990**, *112*, 4192. (h) Tour, J. M.; Wu, R.; Schumm, J. S. *J. Am. Chem. Soc.* **1991**, *113*, 7064. (i) Martin, A. S.; Sambles, J. R.; Ashwell, G. J. *Phys. Rev. Lett.* **1993**, *70*, 218. (j) Pearson, D. L.; Schumm, J. S.; Tour, J. M. *Macromolecules* **1994**, *27*, 2348.

(5) (a) Keller, R. A.; Dolby, L. J. *J. Am. Chem. Soc.* **1969**, *91*, 1293. (b) Breen, D. E.; Keller, R. A. *J. Am. Chem. Soc.* **1968**, *90*, 1935. (c) Kroon, J.; Oliver, A. M.; Paddon-Row: M. N.; Verhoeven, J. W. *J. Am. Chem. Soc.* **1990**, *112*, 4868. (d) Amrein, W.; Schaffner, K. *Helv. Chim. Acta* **1975**, *58*, 397.

(6) Rachele, J. R. *J. Org. Chem.* **1963**, *28*, 2898.

(7) Smith, G. A.; McGimpsey, W. G. *J. Phys. Chem* **1994**, *98*, 2923.

(8) Murov, S. L.; Carmichael, I.; Hug, G. L. *Handbook of Photochemistry* 1992, Marcel Dekker: New York.

(9) Carmichael, I.; Hug, G. L. *J. Phys. Chem. Ref. Data* **1986**, *15*, 1.

(10) Lamola, A. A.; Leermakers, P. A.; Byers, G. W.; Hammond, G. S. *J. Am. Chem. Soc.* **1965**, *87*, 2322.

(11) Chang, D. S. C.; Filipescue, N. *J. Am. Chem. Soc.* **1972**, *94*, 4171.

(12) See (a) Speiser, S. *Chem. Rev.* **1996**, *96*, 1953. (b) Levy, S.-T.; Speiser, S. *J. Chem. Phys.* **1991**, *96*, 3587. (c) Vögtle, F.; Frank, M.; Nieger, M.; Belser, P.; von Zelewsky, A.; Balzani, V.; Barigelletti, F.; De Cola, L.; Flamigni, L. *Angew. Chem., Int. Ed. Engl.* **1993**, *32*, 1643. (d) Sen, A.; Krishnan, V. *Chem. Phys. Lett.* **1998**, *294*, 499. (e) Bravo, J.; Mendicuti, F.; Saiz, E.; Mattice, W. L. *Macromol. Chem. Phys.* **1994**, *195*, 3411. (f) Katayama, H.; Ito, S.; Yamamoto, M. *J. Phys. Chem.* **1992**, *96*, 10115. (g) Kaschke, M.; Ernsting, N. P.; Valeur, B.; Bourson, J. *J. Phys. Chem.* **1990**, *94*, 5757.

(13) See Isied, S. S.; Ogawa, M. Y.; Wishart, J. F. *Chem. Rev.* **1992**, *92*, 381, and references therein.

(14) Schmidt, J. A.; McIntosh, A. R.; Weedon, A. C.; Bolton, J. R.; Connolly, J. S.; Hurley, J. K.; Wasielewski, M. R. *J. Am. Chem. Soc.* **1988**, *110*, 1733.